Journal of Neonatal Surgery
ISSN(Online): 2226-0439
Vol. 13, (2024)
https://www.jneonatalsurg.com

OPEN ACCESS

Role of Lung Ultrasound in Diagnosis of Ventilator Associated Pneumonia

Mohamed Abd-Elkareem Rabea[1], Mona Abdel Hamid Elharrisi[1], Neven Mohamed Gamil[1], Mohamed lofty Mohamed[1],Mohamed Gamal Nada[2]

[1]Anesthesia, Intensive care & Pain management Department, Faculty of Medicine, Zagazig University, Egypt

[2]Diagnostic Radiology Department, Faculty of Medicine, Zagazig University, Egypt

***Corresponding author:**

Mohamed Abd-Elkareem Rabea

Cite this paper as: Mohamed Abd-Elkareem Rabea, Mona Abdel Hamid Elharrisi, Neven Mohamed Gamil, Mohamed lofty Mohamed,Mohamed Gamal Nada, (2024) Role of Lung Ultrasound in Diagnosis of Ventilator Associated Pneumonia. *Journal of Neonatal Surgery*, 13, 1496-1507.

ABSTRACT

Lung ultrasound (LUS) has emerged as a valuable bedside imaging modality in critically ill patients, offering a rapid, non-invasive, and radiation-free alternative to chest X-ray and CT scan. It enables early detection of pulmonary pathologies such as pneumothorax, pleural effusion, pulmonary edema, consolidation, and interstitial syndrome. The increasing accuracy and availability of ultrasound devices have expanded its role in anesthesia, intensive care, and emergency medicine.

Keywords: *Lung ultrasound, ICU, pleural effusion, pneumonia, pulmonary edema, bedside imaging*

1. INTRODUCTION

Lung ultrasound (LUS) has become a valuable imaging modality in the assessment of pulmonary diseases, especially in critically ill patients. It offers a rapid, bedside, and radiation-free method for evaluating lung conditions, allowing clinicians to make prompt and accurate decisions. The ability of ultrasound to visualize pleural and subpleural structures enables early detection of abnormalities such as pneumothorax, pleural effusion, and pulmonary edema, which are common in intensive care settings (1).

In recent years, the diagnostic performance of LUS has been shown to rival or even surpass that of chest radiography for several respiratory conditions. Multiple studies have demonstrated its high sensitivity and specificity for detecting alveolar-interstitial syndrome, consolidations, and pleural pathologies. Furthermore, the portability and safety of ultrasound make it an essential tool in settings where patient transport to radiology is risky or impractical, such as in mechanically ventilated or hemodynamically unstable patients (2).

The integration of lung ultrasound into routine critical care practice aligns with the global movement toward point-of-care ultrasonography (POCUS), emphasizing dynamic, real-time bedside assessment. With appropriate training and standardization, intensivists and anesthesiologists can use LUS not only for diagnosis but also for monitoring disease progression and response to therapy. Thus, lung ultrasound represents a paradigm shift in respiratory evaluation, combining safety, accuracy, and clinical practicality (3).

Lung ultrasound (LUS) was considered unhelpful in the past due to the intrinsic impossibility of the ultrasound to penetrate the air; the only recognized indication was the assessment of pleural effusion. Over the last few years, its usefulness for the clinical management of different diseases has been widely demonstrated. Point-of-care ultrasonography may reduce the use of chest x-rays, computed tomography (CT) scans, and other radiation imaging techniques in the Intensive Care Unit (ICU) and in the Emergency Department (ED). The integration of bedside ultrasonography in the daily clinical activity of intensivists could reduce the risk of radiation exposure, need of patient transport, and hospital costs and may redirect patient's management (4).

Lung ultrasound signs:

Lung examination

Lung ultrasound examination is performed at the bedside in supine position directly by the intensivist. Ultrasound machines are nowadays available in most of the ICUs and both simple and advanced machines are suitable to perform lung ultrasound. For each hemothorax, 6 regions are examined: 3 areas are delimited from the front to the back by sternum and anterior and

posterior axillary lines; each area is divided into a superior and an inferior region (Figure). The choice of the probe depends on patient morphology and suspected pathology. The examination can be started by anterior fields with a high-frequency linear probe, suitable for superficial examination and therefore for the visualization of the pleural line and derived artifacts; the operator can switch to a low-frequency probe (convex or phased-array) if real images are visualized (consolidations, effusions) or the pleural line is too deep to be assessed with a linear probe. A micro-convex probe, if available, is suitable for both types of examination (5).

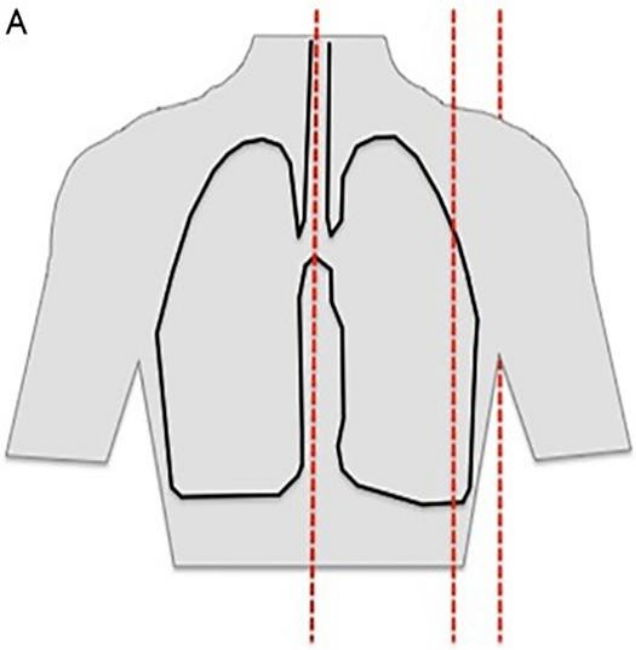

B

AREA	SCORE	Sub-pleural	Air-Bronchogram
L1		☐	☐
L2		☐	☐
L3		☐	☐
L4		☐	☐
L5		☐	☐
L6		☐	☐
R1		☐	☐
R2		☐	☐
R3		☐	☐
R4		☐	☐
R5		☐	☐
R6		☐	☐
TOTAL			

Figure 1: Lung ultrasound examination and report.

(A) Each hemithorax is divided in six regions: 2 anterior, 2 lateral, 2 posteriors, according to anatomical landmarks set by anterior and posterior axillary lines (red dotted lines). Each region is divided in half, superior, and inferior. To perform a comprehensive examination, all adjacent intercostal spaces must be explored in each region of interest, sliding the probe along the space. (B) Examples of simplified report form for rapid reporting and monitoring. For each explored region, the worst finding is reported in simple checkboxes according to the following rating: normal: 0; well-separated B-lines: 1; coalescent B-lines: 2; and consolidation: 3. The cumulative lung ultrasound score corresponds to the sum of each examined region score (minimum score, normal lungs: 0; maximum score, both consolidated lungs: 36). ANT, anterior; INF, inferior; LAT, lateral; POST, posterior; SUP, superior **(6)**

A-lines

In healthy lung, air does not allow ultrasound penetration and only the pleural line is visualized. During tidal ventilation, the lungs expand and the visceral pleura slide against the parietal one, corresponding to a sparkling movement of the pleural line synchronous with inspiration (lung sliding). Beyond this pleural line, regularly spaced motionless horizontal lines (A-lines) are reverberation artifacts of the pleural line; they are generated when lung density is normal. Normal lung aeration is defined by both lung sliding and A-lines **(7)**.

B-lines

Abnormal interlobular septa or alveoli edema provide a gas-tissue interface with the pleural line that alters ultrasound reflection. The result is an ultrasound artifact known as B-line: a hyperechoic laser-shaped vertical artifact arising from the pleural line, moving synchronous with lung sliding, reaching the edge of the screen and erasing the A-lines. B-lines are generated when the lung density increases and are considered significant when ≥3 B-lines are visualized in a scan (B-pattern). ≥3 well-spaced B-lines correspond to moderate lung loss of aeration , whereas coalescent B-lines, resulting from partial filling of alveolar spaces, indicate severe loss of aeration. Those two patterns are classically observed in increased extra vascular lung water either due to increased hydrostatic pressure or altered capillary permeability **(Figure) (8).**

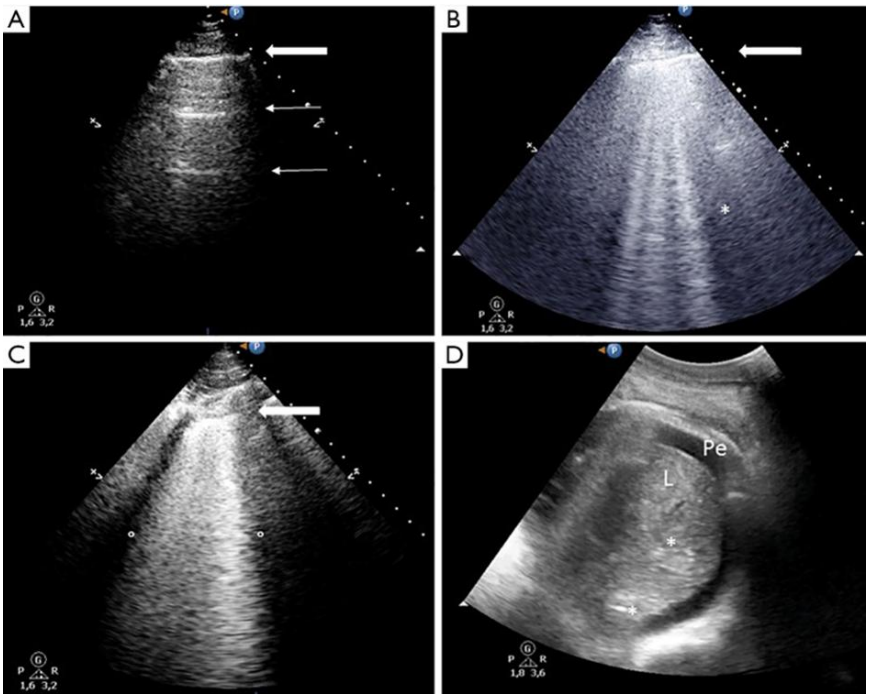

Figure 2: Lung ultrasound score patterns. (A) Normal pattern. The pleural line (white arrow) with multiple horizontal A-lines (thin arrows). (B) The pleural line is visible (white arrow) with separated B-lines (*) arising from the pleural line and spreading up to the edge of the screen. (C) The pleural line is visible (white arrow) with coalescent B-lines (between °) arising from the pleural line and spreading up to the edge of the screen. (D) Transversal view of a consolidated lower lobe **(6)**

Lung consolidation

Lung lobar/hemilobar consolidations are visualized when the loss of aeration is complete and the lung appears as a tissue-like structure. Lung consolidations have a well-delimited external margin, while the inner limit can be either irregular if aerated lung is in continuity or regular in case of complete lobe consolidation. Within consolidations, air-bronchograms are visualized as hyperechoic images. During inspiration, penetration of gas through the bronchial tree into consolidations reinforces their appearance, giving a dynamic air-bronchogram. A dynamic air-bronchogram allows ruling out obstructive atelectasis. If the air-bronchogram is static or absent, it suggests non-patent airways: however, it is not specific for a diagnosis. Air-bronchogram morphology (punctiform or linear/arborescent) may provide additional information for further differential diagnosis of consolidations **(Figure) (9).**

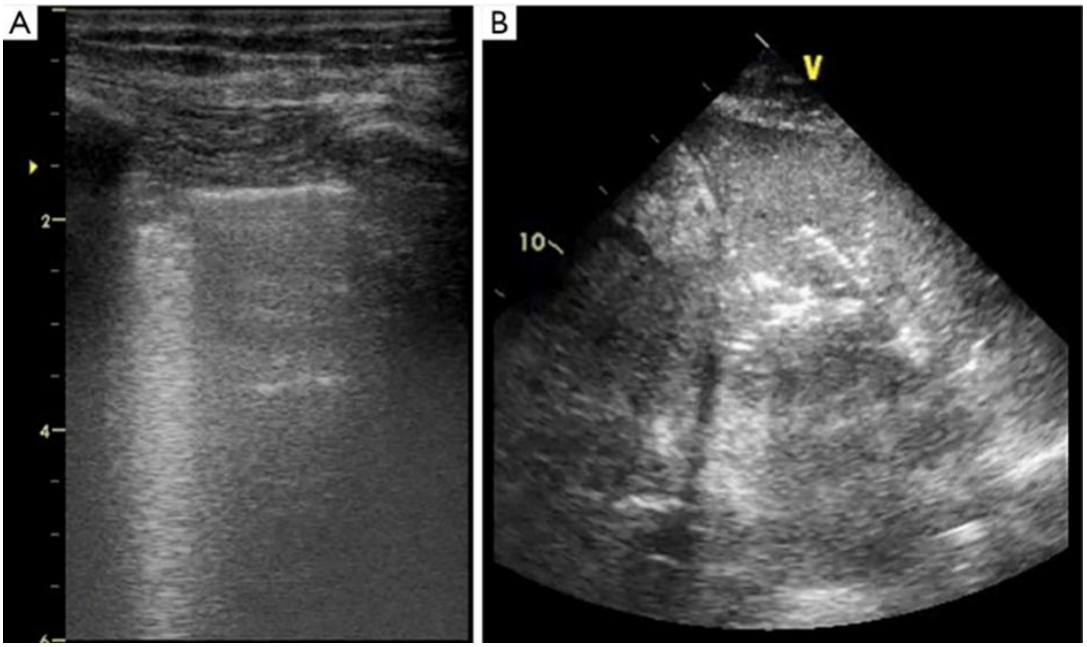

Figure 3: Lung ultrasound signs of consolidation . (A) A sub pleural consolidation is visualized on the left as an echopoor image juxtaposed to the pleura and generating hyperechoic artifacts (longitudinal scan – linear probe). (B) Within a consolidated lung, a dynamic arborescent air-bronchogram is visualized as a hyperechoic image moving synchronous with tidal ventilation and shaping the bronchial tree **(6)Radiographic correlation of lung US findings**

Air-filled lung

The A-line artifact predominates in normal air-filled lungs **(Figure)**. In addition, during respiration the sliding visceral and parietal pleura is visualized as shimmering motion of the pleural line, referred to as *lung sliding*. Pathologic conditions with air-filled lungs also have A-line artifacts; these conditions include asthma, chronic obstructive pulmonary disease, mild viral illness, and pulmonary embolism without focal infarct. In suspected pulmonary embolism, in which A-lines predominate, a US examination of the deep venous structures can be performed. In addition, if a pulmonary infarct is present, it will appear as a consolidation abutting the pleural surface **(10)**.

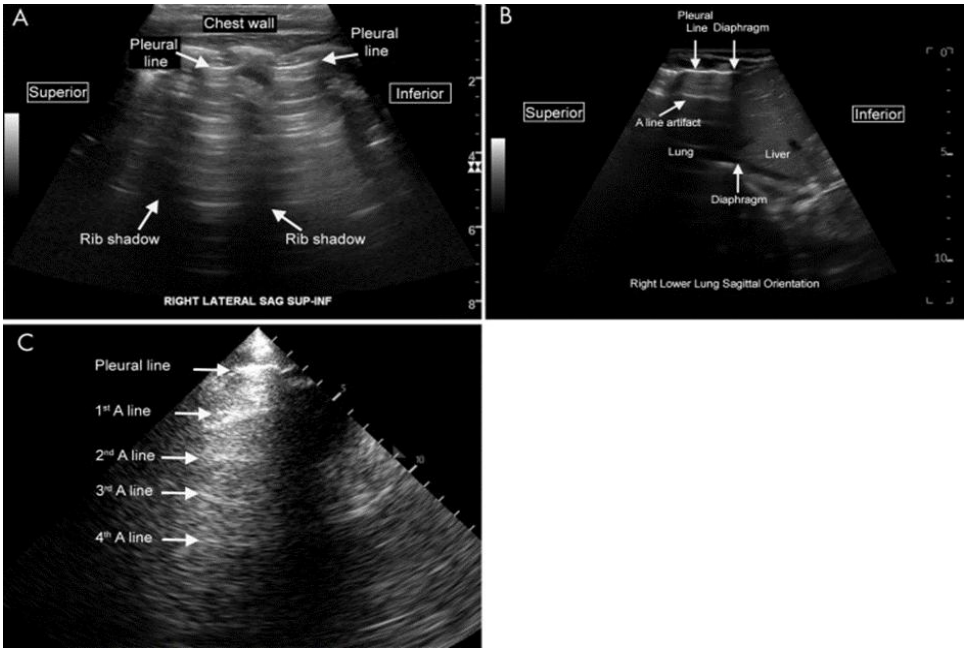

Figure 4: Normal lung US anatomy. *A,* Labeled US image of normal lung in a pediatric patient (scanning performed in the sagittal orientation with a curvilinear abdominal probe). The pleural line is the labeled hyperechoic line that represents the junction of the visceral and the parietal pleura. The A-line artifacts are clearly visualized as horizontal reverberation artifacts of the hyperechoic pleural line. The rib shadows separate the intercostal spaces. *B,* Labeled US image of normal lung in a neonate (scanning performed in the sagittal orientation at the lower lung). The interface between the liver and lung is clearly visualized. *C,* Labeled lung image from a lower-end ultrasound machine with a suboptimal acoustic window. Even on such limited examinations, normal A-line artifact can often still be appreciated on careful examination, as seen here **(11)**

Interstitial thickening: edema and fibrosis

When the pulmonary interstitium thickens (secondary to fibrosis or fluid), B-line artifacts replace the normal A-lines. B-line artifact consists of well-defined, laserlike, vertical, echogenic lines arising from the pleural line and extending to the bottom of the image. Scattered B-lines (fewer than two per intercostal space) can be present in normal lung. The number of B-lines directly correlates to disease severity. B-lines are diffusely present in the setting of pulmonary edema, pulmonary fibrosis, and pneumonitis (including vaping injury) **(Figure -Figure)**. The presence of B-lines on US is sensitive for pulmonary edema and may be more sensitive compared to chest radiography for its detection. Focal and/or unilateral B-lines suggest a localized process such as atypical pneumonia **(12)**.

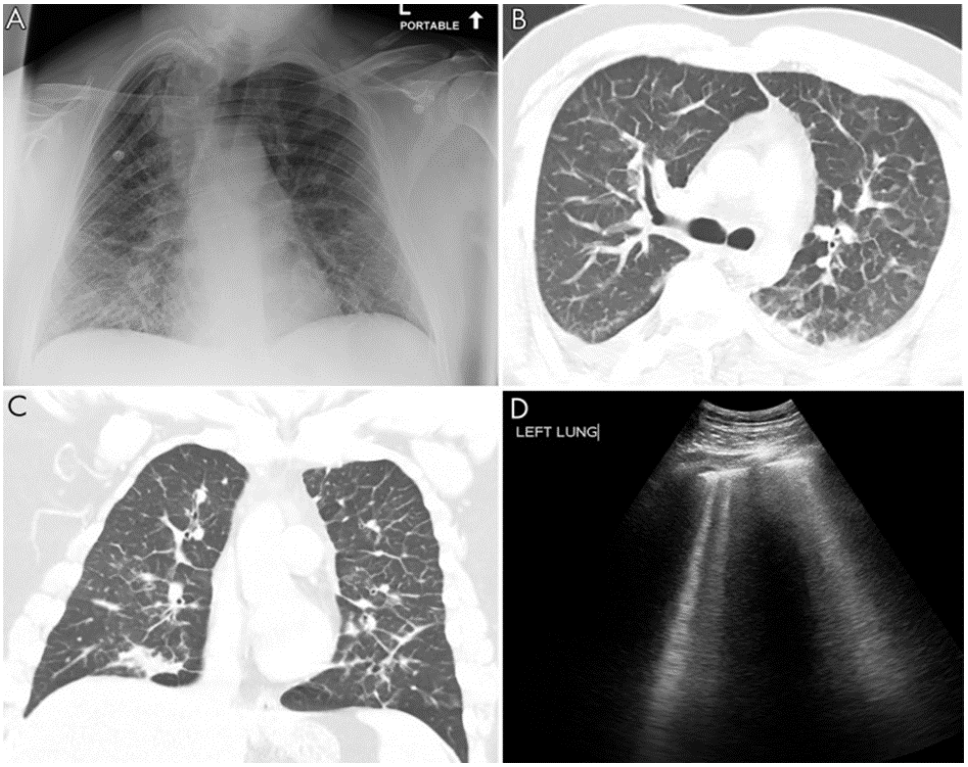

Figure 5: Pulmonary edema on lung US. *A,* Anteroposterior chest radiograph shows nonspecific prominent interstitial markings bilaterally in a 27-year-old man with pulmonary edema. *B,* Axial and *C,* coronal CT images show marked bilateral septal thickening, scattered consolidation, and ground-glass opacity. *D,* Lung US shows B-line artifacts arising from the pleural line and loss of A-lines **(11)**

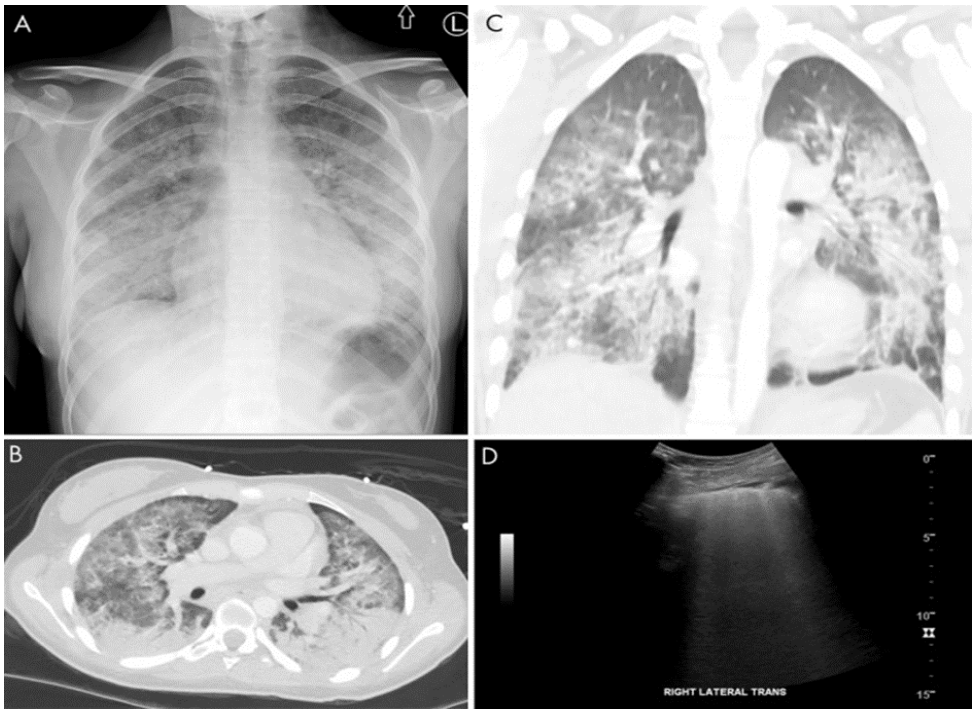

Figure 6: Vaping lung injury on lung US. *A,* Anteroposterior chest radiograph demonstrates nonspecific bilateral interstitial and consolidative pulmonary opacity in a 17-year-old adolescent girl with a vaping-induced lung injury. *B,* Axial and *C,* coronal CT images demonstrate diffuse bilateral consolidation, interstitial thickening, and ground-glass opacity. *D,* Lung US demonstrates loss of A-lines with confluent B-line artifacts better appreciated on the cine clip **(11)**.

Pneumothorax

A pneumothorax separates the visceral and parietal pleura, eliminating normal lung sliding between these layers on lung US. The point of transition between the pneumothorax and normal lung is known as the lung point. Identification of a lung point on lung US yields 100% specificity for pneumothorax. Pneumothorax can also be identified at M-mode US, a technique that depicts motion. In a healthy lung, the tissue superficial to the pleural line remains stationary, with smooth horizontal lines at M-mode imaging. Deep to the pleura, the lung motion interrupts the lines, creating a finely interrupted granular or "sandy" pattern. This normal pattern is called the seashore sign as it depicts the boundary between the stationary chest wall ("ocean") and moving lung ("sand") **(Figure)**. When a pneumothorax is examined at M-mode US, the smooth horizontal lines are uninterrupted, as the chest wall and air deep to the pleura are both stationary in pneumothorax. This appearance of pneumothorax at M-mode examination has been dubbed the bar code sign **(Figure).** Lung US surpasses chest radiography in sensitivity for pneumothorax. The addition of color Doppler US can improve detection of pneumothorax, as color signal from the lung is absent owing to the air barrier of the pneumothorax **(13)**.

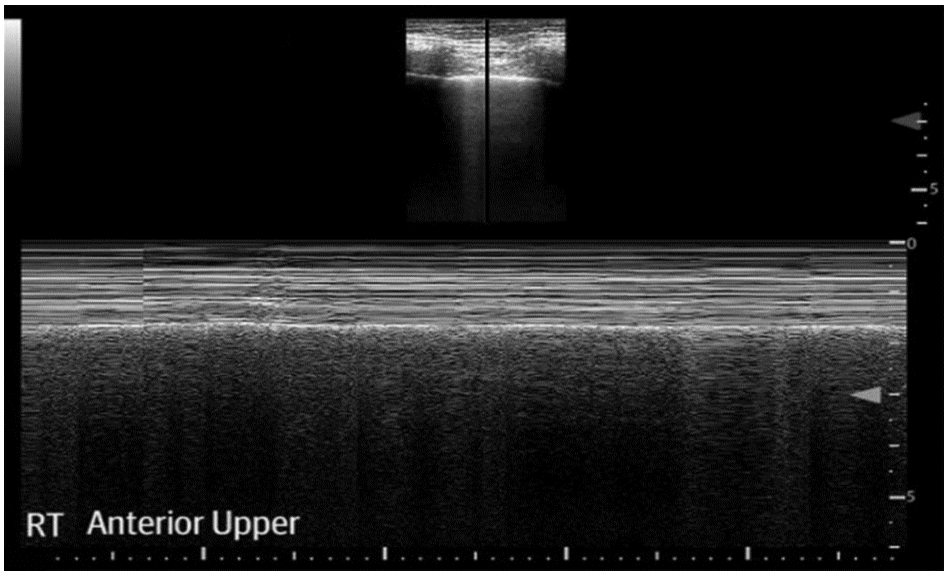

Figure 7: In healthy lung, M-mode US shows the seashore sign in which tissue superficial to the pleural line remains stationary creating smooth horizontal lines, and deep to the pleura, the lung motion interrupts the lines, creating a finely interrupted granular or "sandy" pattern. RT = right **(11)**

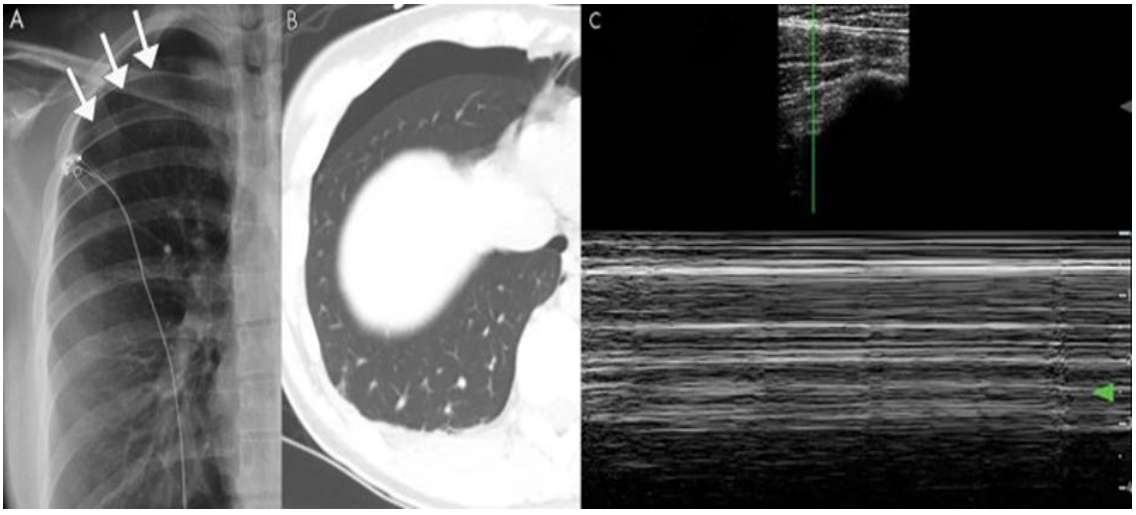

Figure 8: Pneumothorax on lung US. *A,* Posteroanterior chest radiograph and *B,* axial CT image of a spontaneous pneumothorax in a 26-year-old patient. *C,* M-mode US image shows the barcode sign, in which the smooth horizontal lines corresponding to the stationary chest wall are uninterrupted owing to lack of lung sliding, which is diagnostic for pneumothorax **(11)**

Pleural effusion

US directly images pleural fluid. Simple effusions commonly present as anechoic fluid in the posterior dependent lung. Complex pleural fluid collections, including chronic effusions, malignant effusions, hemothorax, and empyema, are more heterogeneous in appearance on US depending on extent of debris, septations, and pleural thickening. Given the ability to visualize this level of detail, lung US is often better than conventional chest radiography for assessing complicated pleural effusions and assists in interventional management. Lung US can help to identify loculated areas for drainage or indicate the need for more aggressive therapy, including surgical washout or tissue plasminogen activator administration. A large effusion creates an acoustic window, allowing visualization of the vertebral bodies, also known as the spine sign **(Figure) (14).**

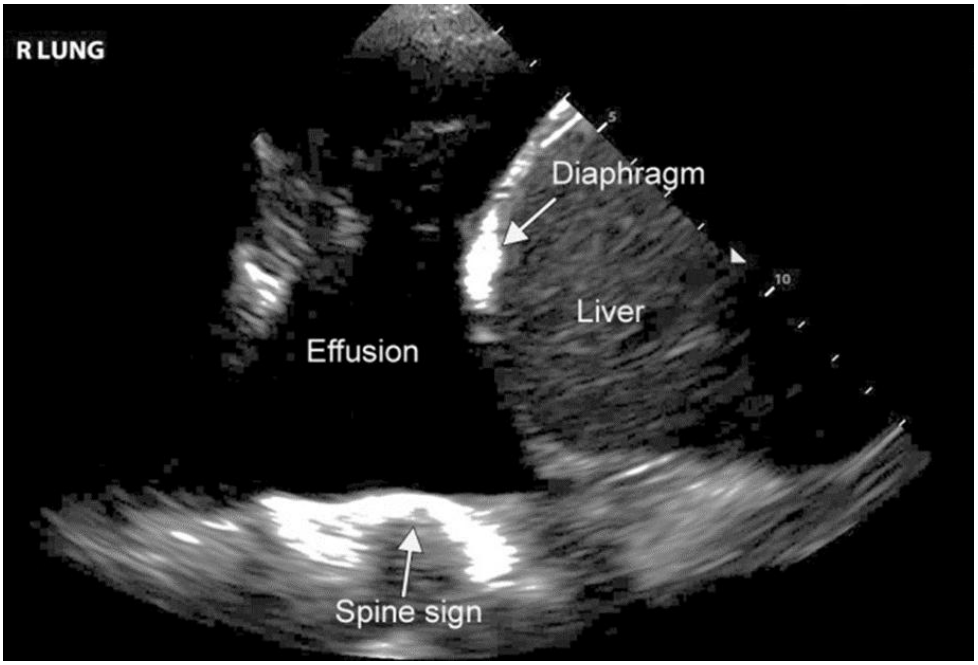

Figure 9: Pleural effusion on lung US. Lung US image of a patient with a moderate-sized pleural effusion. The acoustic window created by the effusion allows visualization of the spine (spine sign), as can be seen in this image. Normally, the vertebral bodies are not apparent on US **(11).**

Infection

Lung US is an excellent modality to evaluate and monitor known or suspected pulmonary infection. Pneumonia has several imaging appearances depending on the extent of consolidation or interstitial involvement. A completely consolidated lung mimics the solid appearance of the liver; this is known as hepatization **(Figure 1)**. In consolidation, fluid or cells fill the alveoli, and the normal A-lines or air-filled lung are lost. If air bronchograms are present, they are manifested as hyperechoic foci within the consolidated lung (**Figure 1**). The interface between consolidated abnormal lung and aerated normal lung is identified by an irregular hyperechoic line termed the shred sign (**Figure 1**) **(15)**.

Smaller infections may manifest as a focal subpleural hypoechoic area. In early infection, focal B-lines may be present, indicating that the affected interstitium is becoming thickened and/or inflamed. Color Doppler imaging is useful for the evaluation of lung abscesses and empyema. A lung abscess demonstrates internal vascularity, because there are residual portions of the necrotic lung parenchyma in the lesion **(Figure 2)**. In comparison, pleural-based empyema demonstrates no internal flow **(Figure 3)**. Foci of gas within a collection are hyperechoic and demonstrate twinkle artifact on color Doppler US. Complex conditions containing mixed areas of pneumonia, atelectasis, and pleural fluid often are better assessed at lung US than at chest radiography **(Figure 4) (16)**.

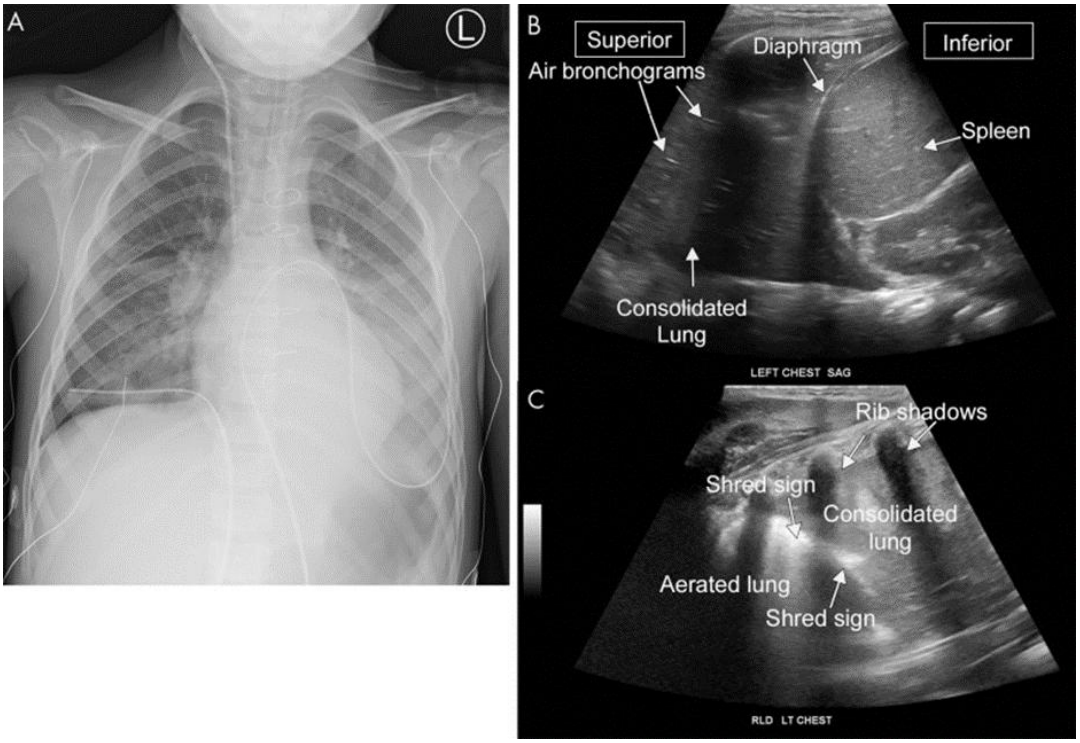

Figure 1: Pneumonia on lung US. *A,* Anteroposterior chest radiograph and *B, C,* US images from a 6-year-old patient with pneumonia. The lower lung on US appears similar in appearance to the liver, representing so-called hepatization of the pulmonary parenchyma consistent with consolidation. *B,* the hyperechoic foci within the consolidation are air bronchograms. *C,* the shred sign is the irregular hyperechoic line separating the consolidated and aerated lung **(11)**

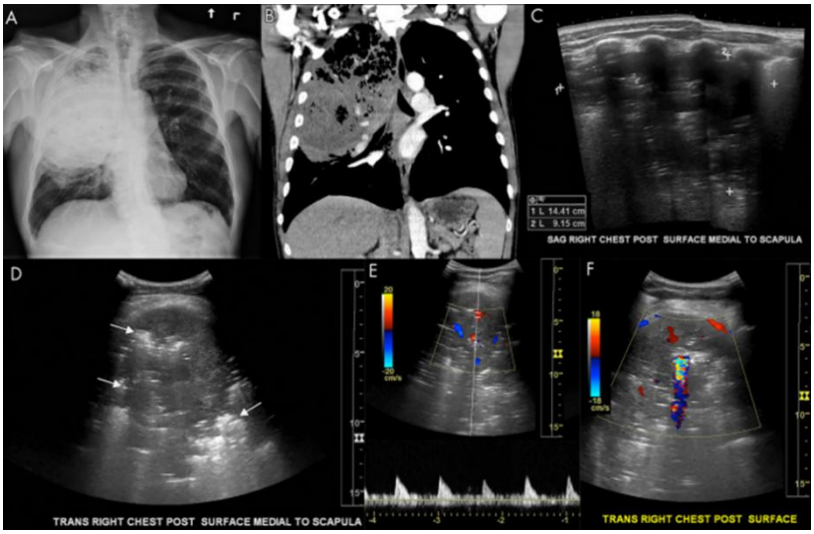

Figure 2: Pulmonary abscess on lung US. *A,* Anteroposterior chest radiograph and *B,* coronal chest CT image show a large pulmonary abscess in the right upper lung containing foci of air in a 56-year-old smoker. *C,* Sagittal and *D,* transverse grayscale US images demonstrate a large 14-cm abscess. Hyperechoic foci are seen throughout the abscess corresponding to air (arrows, *D*). *E, F,* Associated color Doppler images show internal Doppler flow consistent with abscess. There is a large focus of twinkle artifact corresponding to air within the abscess (dashed arrow, *F*) **(11)**.

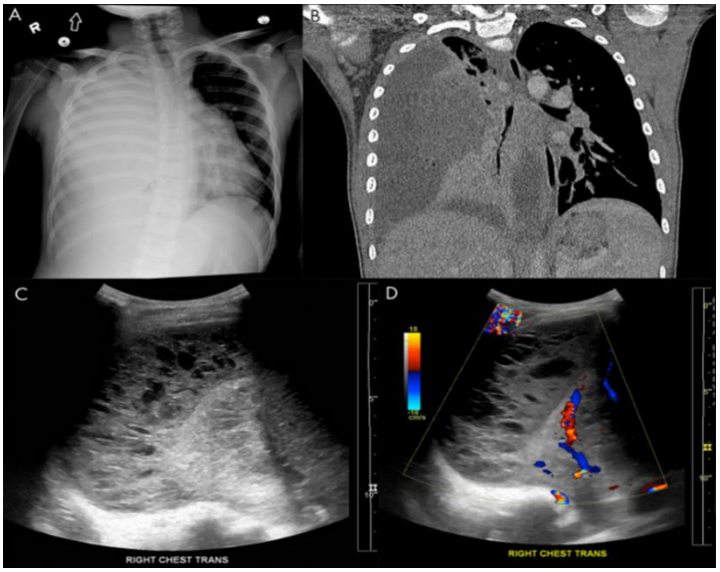

Figure 3: Empyema on lung US. ***A,*** Anteroposterior chest radiograph and *B,* coronal chest CT image show a large, right-sided empyema occupying the pleural space with associated compression of the pulmonary parenchyma in a 9-year-old boy. Lung US *C,* grayscale and *D,* Doppler images demonstrate a multiloculated complex-appearing fluid collection in the pleural space with septations and internal debris without internal color flow **(11)**

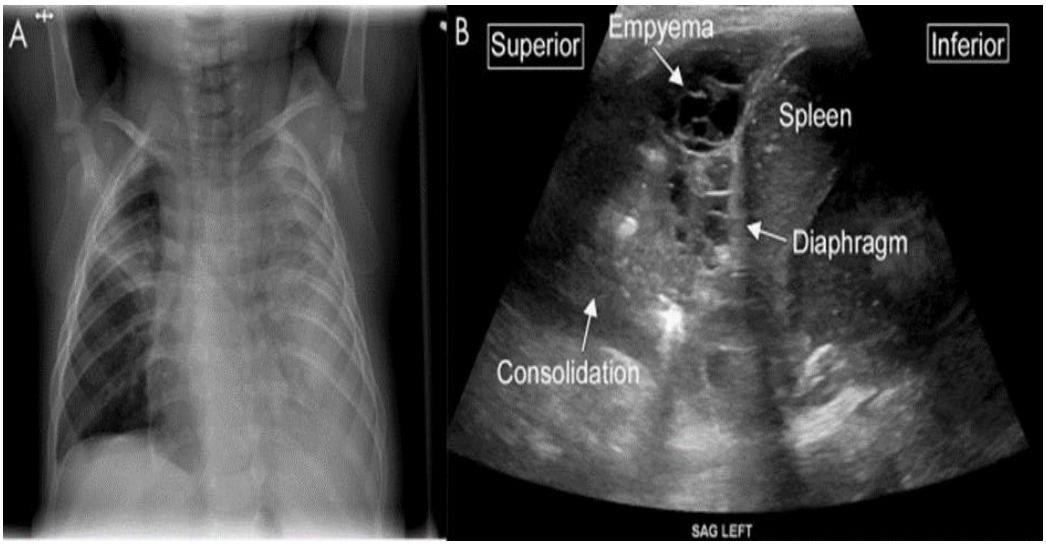

Figure 4: Complex collection on lung US. *A,* Anteroposterior chest radiograph demonstrates near complete opacification of the left hemothorax, with loculated pleural fluid tracking along the left lateral chest wall in an 8-month-old male infant. In addition, a focal consolidation is present in the right upper lobe. *B,* Sagittal US image from the same patient shows consolidation within the lung and a multiseptated complex pleural fluid collection consistent with empyema **(11)**

Viral infections, including COVID-19 and bronchiolitis, can also be assessed and monitored using lung US. There is subjective enthusiasm for the ability of lung US to diagnose, stratify risk, and monitor COVID-19 infection, although findings at lung US can lack specificity. B-line artifact of varying severity, consolidations, and pleural irregularities have all been visualized in COVID-19 infection **(Figure 5)**. In areas of focal ground-glass opacity, diffuse confluent B-lines are present with loss of A-lines. Pleural effusion is rare in these patients. During the recovery phase, the B-lines decrease and the A-lines typically return. It is important to note that lung US performed on patients with COVID-19 presents a risk to the operator; this risk can be minimized with the proper use of protective equipment. Outside of COVID-19, lung US is effective in evaluating viral infection in pediatric patients **(17)**.

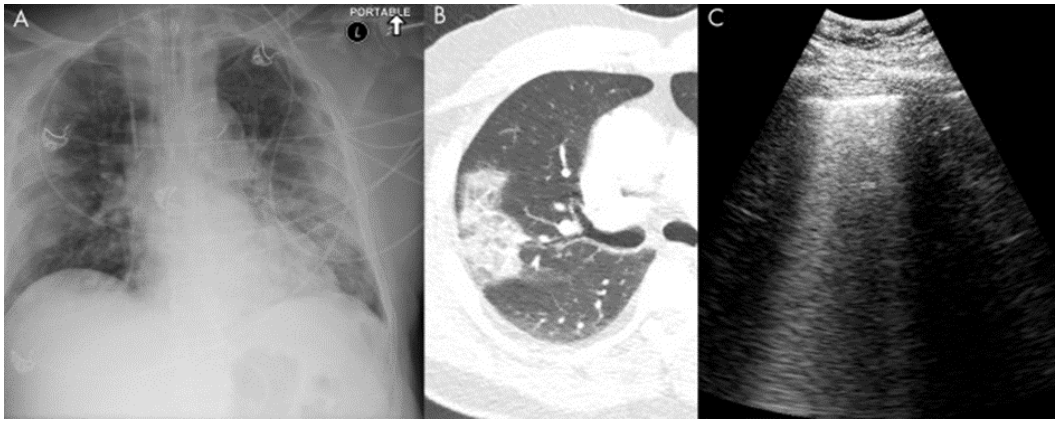

Figure 5: COVID-19 infection on lung US. *A,* Anteroposterior chest radiograph, *B,* axial chest CT image, and *C,* lung US image from the same 74-year-old man, who tested positive for COVID-19 5 days prior to imaging. The chest radiograph shows bilateral peripheral opacity, which presents with a ground-glass appearance on the chest CT image. Lung US imaging in this patient demonstrated numerous B-lines throughout the parenchyma which were diffusely confluent in some sections **(11)**

Lung ultrasound for VAP diagnosis

Concerning LUS signs, the presence of a tissue-like pattern alone had 93% sensitivity but 0% specificity, thus confirming that other etiologies than VAP may induce complete loss of aeration in mechanically ventilated patients. On the contrary, the visualization of one consolidated region with linear/arborescent dynamic air-bronchogram showed greater specificity (81%). Subpleural consolidations resulted to be a sensible sign, with limited specificity **(Table) (18)**.

Table 1: Ventilator-associated pneumonia lung ultrasound score (VPLUS) (6)

Parameter	VPLUS
Purulent tracheal secretions	1
≥ Areas with subpleural consolidations	1
≥ Area with dynamic linear/arborescent air-bronchogram	2
EA positive quantitative/qualitative culture*	1

*, additional parameters to be added in for modified versions of the score. EA, endotracheal aspirate.

In pathology, disseminated associated VAP injuries extend from the centre to the periphery. Wherever those lesions reach the pleural line, they become identifiable by LUS. As VAP extends, normal pattern is replaced by focal areas of interstitial syndrome represented by well-spaced B lines, progressively becoming confluent; this is then replaced by small sub pleural consolidations, disseminated to anterior and lateral chest wall. If not treated, those small consolidations merge to become larger lobar consolidation. The air-bronchogram might be visualized within large consolidations. Being VAP an evolutive process reaching the chest wall, lung ultrasound examination seems to perfectly match VAP diagnosis features. However, despite the description of specific ultrasound patterns for VAP, to this day, a prospective application of LUS signs in early VAP diagnosis is lacking. Because many VAP occurs in already injured regions, it was believed that the LUS examination should focus on lesions evolution rather than on appearance of new lesions **(16)**.

Once diagnosed, LUS can also be used to monitor VAP recovery and antibiotic efficacy. Effective treatment should result in progressive disappearance of VAP signs whereas when inappropriately treated, subpleural consolidations are expected to keep appearing and to extend. For this purpose, a LUS score can be used to quantify the global loss of aeration and monitor its modification in days. An aeration score is attributed to each of the 12 standard regions: 0 if A-lines or maximum 2 B-lines are visualized, score 1: ≥3 B-lines (well-spaced or involving ≤50% of the pleura, depending on the approach), score 2: B-lines becoming coalescent or involving >50% of the pleura, score 3: tissue-like pattern. The global LUS score is computed

as the sum of the regional scores **(19)**.

A regional re-aeration score can be computed in each area to monitor the effectiveness of a treatment aiming at increasing lung aeration, as antibiotics in VAP or recruitment maneuvers: the aeration improvement will give a positive score of +1, +3 or +5 points if a switch of 1, 2 or 3 steps in LUS score is observed. A worsening in lung aeration will give a negative score of −1, −3 or −5 points is a switch of 1, 2 or 3 steps is remarked. The global re-aeration score is computed as the sum of each regional re-aeration score. When computed after 7 days of antibiotics in VAP patients, global LUS re-aeration score showed a significant correlation with re-aeration as assessed by quantitative CT scan. A systematic approach for diagnosis and monitoring of VAP with LUS is proposed in **Figure (20)**.

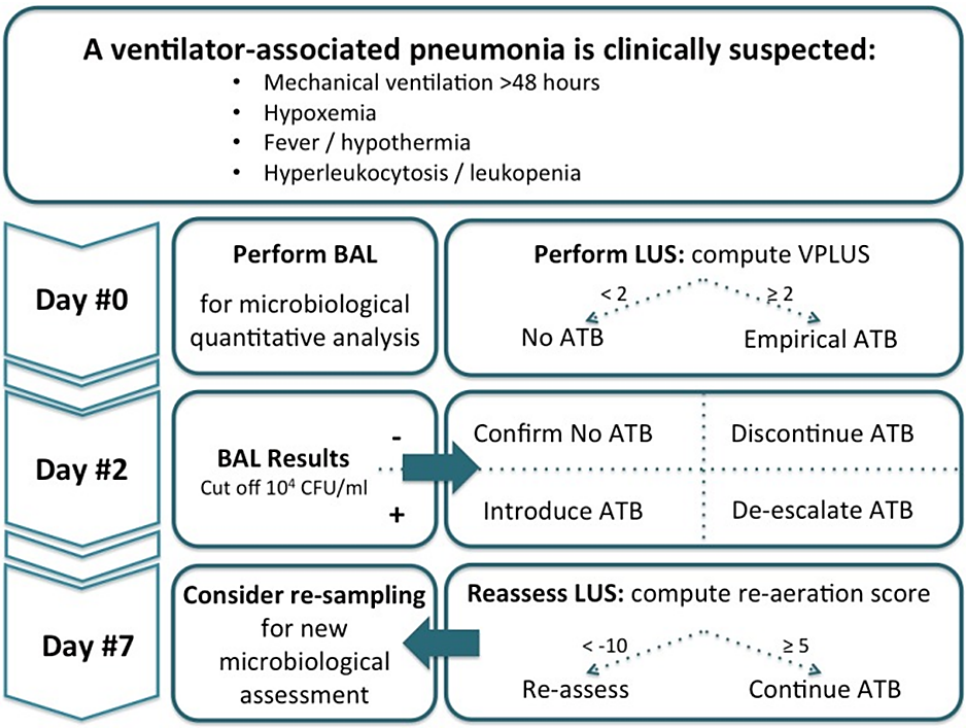

Figure 15:A systematic approach for diagnosis and monitoring of ventilator-associated pneumonia. BAL, broncho-alveolar lavage; ATB, antibiotics; VPLUS, ventilator-associated pneumonia lung ultrasound score; LUS, lung ultrasound **(6)**

2. LIMITATIONS OF LUS

Classical limitations in LUS application are the presence of subcutaneous emphysema or thoracic dressings, since preventing ultrasound penetration. For the specific application of VAP diagnosis and monitoring, although previous study suggested the presence of specific and sensible ultrasound signs, a prospective application is still lacking. Moreover, while the dynamic linear/arborescent air-bronchogram is a specific sign, it's poorly sensible and false negative exist; a second LUS examination after disobstructive fiber-bronchoscopy has been suggested to detect previously masked air-bronchogram, but still has to be confirmed in a wider population **(21)**..

REFERENCES

[1] Volpicelli, G., Lamorte, A., Villén, T. (2020). What's new in lung ultrasound during the COVID-19 pandemic. Intensive Care Medicine, 46(7), 1445–1448. https://doi.org/10.1007/s00134-020-06182-0

[2] Soldati, G., Smargiassi, A., Inchingolo, R., et al. (2021). Lung ultrasonography in critical care and emergency medicine: A practical guide. Respiration, 100(9), 870–880. https://doi.org/10.1159/000515251

[3] Mento, F., Perrone, T., Tursi, F., & Smargiassi, A. (2023). Advances in point-of-care lung ultrasound for critically ill patients. Diagnostics, 13(3), 459. https://doi.org/10.3390/diagnostics13030459

[4] Mojoli, F., Bouhemad, B., Mongodi, S. & Lichtenstein, D. 2019. Lung ultrasound for critically ill patients. Am J Respir Crit Care Med, 199, 701-14.

[5] Morgan, S. 2022. Respiratory assessment: undertaking a physical examination of the chest in adults. Nurs Stand, 37, 75-82.

[6] Bouhemad, B., Dransart-Rayé, O., Mojoli, F. & Mongodi, S. 2018. Lung ultrasound for diagnosis and monitoring of ventilator-associated pneumonia. Ann Transl Med, 6, 418.

[7] Xing, W., Li, G., He, C., Huang, Q., Cui, X., Li, Q., et al. 2023. Automatic detection of A-line in lung ultrasound images using deep learning and image processing. Med Phys, 50, 330-43.

[8] Rigot, M., Boysen, S. R., Masseau, I. & Letendre, J. A. 2024. Evaluation of B-lines with 2 point-of-care lung ultrasound protocols in cats with radiographically normal lungs. J Vet Emerg Crit Care (San Antonio), 34, 143-52.

[9] Churchill, L. J., Tronstad, O., Mandrusiak, A. M., Waldmann, J. Y. & Thomas, P. J. 2024. The role of lung ultrasound for detecting atelectasis, consolidation, and/or pneumonia in the adult cardiac surgery population: A scoping review of the literature. Aust Crit Care, 37, 193-201.

[10] Green, D. B., Wallace, A. B., Restrepo, C. S., Merrick, D. T., Raptis, D. A., Bhalla, S., et al. 2021. Fluid-filled cystic lesions of the lungs. J Thorac Imaging, 36, 208-17.

[11] Marini, T. J., Rubens, D. J., Zhao, Y. T., Weis, J., O'Connor, T. P., Novak, W. H., et al. 2021. Lung ultrasound: The essentials. Radiol Cardiothorac Imaging, 3, 20-30.

[12] Lichtenstein, D. A. 2019. Current misconceptions in lung ultrasound: A short guide for experts. Chest, 156, 21-5.

[13] Montgomery, S., Li, F., Funk, C., Peethumangsin, E., Morris, M., Anderson, J. T., et al. 2023. Detection of pneumothorax on ultrasound using artificial intelligence. J Trauma Acute Care Surg, 94, 379-84.

[14] Shao, R. J., Du, M. J. & Xie, J. T. 2022. Use of lung ultrasound for the diagnosis and treatment of pleural effusion. Eur Rev Med Pharmacol Sci, 26, 8771-6.

[15] Lovrenski, J. 2020. Pediatric lung ultrasound - pros and potentials. Pediatr Radiol, 50, 306-13.

[16] Boccatonda, A., Cocco, G., D'Ardes, D., Delli Pizzi, A., Vidili, G., De Molo, C., et al. 2023. Infectious pneumonia and lung ultrasound: A review. J Clin Med, 12, 11-22.

[17] Gargani, L., Soliman-Aboumarie, H., Volpicelli, G., Corradi, F., Pastore, M. C. & Cameli, M. 2020. Why, when, and how to use lung ultrasound during the COVID-19 pandemic: enthusiasm and caution. Eur Heart J Cardiovasc Imaging, 21, 941-8.

[18] Di Serafino, M., Dell'Aversano Orabona, G., Caruso, M., Camillo, C., Viscardi, D., Iacobellis, F., et al. 2023. Point-of-care lung ultrasound in the intensive care unit-the dark side of radiology: Where do we stand? J Pers Med, 13, 11-22.

[19] Mongodi, S., De Vita, N., Salve, G., Bonaiti, S., Daverio, F., Cavagnino, M., et al. 2022. The role of lung ultrasound monitoring in early detection of ventilator-associated pneumonia in COVID-19 patients: a retrospective observational study. J Clin Med, 11.

[20] García-de-Acilu, M., Santafé, M. & Roca, O. 2023. Use of thoracic ultrasound in acute respiratory distress syndrome. Ann Transl Med, 11, 320-99.

[21] Di Pietro, S., Mascolo, M., Falaschi, F., Brambilla, W., Ruzga, R., Mongodi, S., et al. 2021. Lung-ultrasound objective structured assessment of technical skills (LUS-OSAUS): utility in the assessment of lung-ultrasound trained medical undergraduates. J Ultrasound, 24, 57-65.